Magnetic-field-induced intersubband resonances in AlGaAs/GaAs quantum wells

C Gauer, Achim Wixforth, Jörg P. Kotthaus, G Abstreiter, G Weimann, W Schlapp

Angaben zur Veröffentlichung / Publication details:

Gauer, C, Achim Wixforth, Jörg P. Kotthaus, G Abstreiter, G Weimann, and W Schlapp. 1995. "Magnetic-field-induced intersubband resonances in AlGaAs/GaAs quantum wells." *Europhysics Letters (EPL)* 30 (2): 111–16. https://doi.org/10.1209/0295-5075/30/2/009.

Magnetic-Field–Induced Intersubband Resonances in AlGaAs/GaAs Quantum Wells.

C. GAUER (*), A. WIXFORTH (*), J. P. KOTTHAUS (*), G. ABSTREITER (**)
G. WEIMANN (**) and W. SCHLAPP (***)

(*) *Sektion Physik der Ludwig-Maximilians-Universität München*
Geschwister-Scholl-Platz 1, D-80539 München, Germany
(**) *Walter Schottky Institut, Technische Universität München*
D-85748 Garching, Germany
(***) *Forschungsinstitut der Deutschen Bundespost*
Postfach 5000, D-64259 Darmstadt, Germany

Abstract. – We present a mechanism to excite intersubband transitions at normal incidence in quantum wells with a magnetic field applied parallel to the two-dimensional electron gas. In the Voigt configuration the light polarization perpendicular to the magnetic field induces intersubband transitions whose oscillator strength is proportional to the square of the field. This dependence allows us to determine experimentally the intersubband matrix elements with great accuracy.

In the past few years enormous progress has been made in the field of infrared detectors based on transitions between electrical subbands in quantum confined semiconductor structures. Both high detectivity as well as the feasibility of large-array detectors have been successfully demonstrated (for a review see [1]). So far, the material combination exhibiting superior device performance is certainly AlGaAs/GaAs although other systems are being increasingly investigated [2].

The high symmetry of the conduction band structure of III/V semiconductor heterojunctions such as AlGaAs/GaAs gives rise to a polarization selection rule stating that intersubband resonances (ISR) can only be excited with the radiation transverse to the plane of the two-dimensional electron gas [3]. Therefore light impinging normally onto the sample surface will not excite intersubband transitions. Because of this selection rule conventional intersubband absorption experiments are usually carried out in one of the following configurations: First, the sample can be tilted at an oblique angle with respect to the optical path [4], but this yields only a small transverse electric-field component resulting in a weak absorption. Secondly and more efficiently, ISR can be excited using metallic grating couplers [5] which provide a substantial electric field parallel to the direction of confinement.

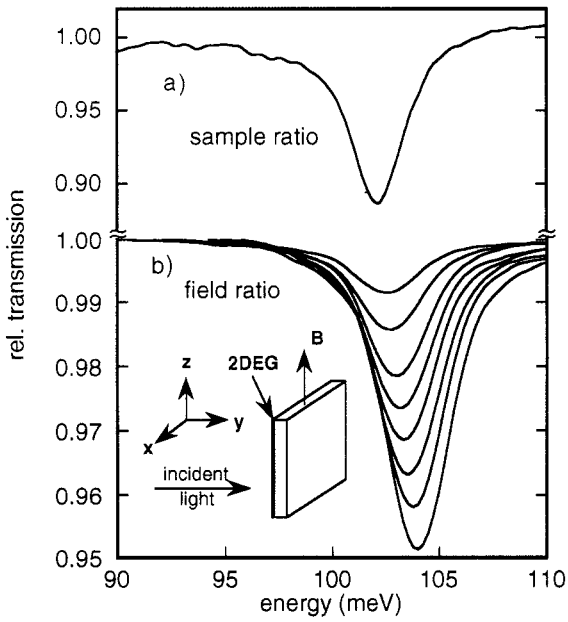

Fig. 1. – Spectrum of sample I (*a*)) taken with the radiation incident under an oblique angle of 63° in the sample ratio. The strength of the resonance observed in this configuration follows the same polarization dependence as expected for intersubband transitions. Relative transmission spectra $T(B \neq 0)/T(B = 0)$ of the same sample in the Voigt configuration at magnetic fields $B = 6$ T, 8 T, 10 T, 11 T, 12 T, 13 T, 14 T, and 15 T (*b*)). The resonance vanishes at zero field and gains oscillator strength with magnetic field. The shift of the resonance position can be explained in terms of the diamagnetic shift. The inset shows a schematic of the experimental geometry.

Finally, strong absorption is also achieved in quantum well wave guides [6] where the light is coupled via the edge of the sample and then reflected several times at the metallized surfaces.

Here, we present an alternative way to excite ISR by applying a magnetic field parallel to the quantum well plane while the light is incident normally. In this geometry («Voigt configuration», see inset of fig. 1*b*)) the magnetic and electrical confinements hybridize into so-called magneto-electric subbands [7]. We show that the presence of the parallel magnetic field gives rise to allowed transitions between these hybrid subbands. By measuring the magnetic-field dependence of the ISR we can determine the relevant matrix elements very accurately and obtain good agreement with our experimental results measured under oblique incidence. Also, good agreement is achieved with theoretical predictions based on an 8-band model. One-band calculations are also effective, but only if the increase of the electronic mass at high energies is properly taken into account. Furthermore, we can explain the experimentally observed diamagnetic shift of the resonances in terms of the 8-band model.

We investigated two different AlGaAs/GaAs multi-quantum well structures (samples I and II) of different well width whose characteristics are given in table I. The mid infrared spectra were recorded using a rapid-scan Fourier-transform spectrometer with the samples mounted in the Voigt geometry at the centre of a superconducting solenoid. We determined the relative change in transmission $T(B \neq 0)/T(B = 0)$ of the unpolarized radiation using a copper-doped germanium photoconductor as a detector. Alternatively, we could ratio against

TABLE I.

	Sample I	Sample II
N_s (10^{12} cm^{-2}) at 77 K	0.63	0.824
number of wells	30	25
well width (Å)	95	59
barrier width (Å)	441	363
doped part of barrier (Å)	98	81
Si: doping (cm^{-3})	0.714	1.68
nominal Si density (cm^{-2})	0.699	1.36
Al concentration	0.349	0.354
μ (cm^2/Vs) at 77 K	57 000	28 765
E_{10} (meV) (calculated)	96	163.9
E_{10} (meV) (measured)	102.1	158.4

the spectrum of a reference substrate. All experiments were performed at low temperatures $T \approx 4$ K.

A transmission spectrum of sample I taken under an oblique angle of 63° is shown in fig. 1*a*). The energy of the observed resonance agrees well with the calculated value of the ISR and also the polarization dependence of the oscillator strength corresponds to that of an ISR. In fig. 1*b*) we show the relative transmission spectra of the same sample in the Voigt configuration at in-plane magnetic fields up to 15 T. In this geometry, there is no intersubband absorption at $B = 0$ T as confirmed by ratioing against a reference substrate. We thus conclude that the observed transitions are induced by the in-plane magnetic field. The oscillator strength, as extracted from the area under the resonance curves, increases strongly with the applied magnetic field and the resonance energies rise. Comparing the spectra shown in fig. 1*a*) and *b*) leads us to interpret the resonances in the Voigt configuration also as intersubband transitions.

We now address the question as to why the in-plane magnetic field breaks the polarization selection rule stated above. To this end, we calculate the dipole matrix element $\langle 1 | H_{\text{int}} | 0 \rangle$ including a finite in-plane magnetic field in the interaction Hamiltonian $H_{\text{int}} = (e/m^*)\,\boldsymbol{\alpha}\boldsymbol{P}$, where $\boldsymbol{P}$ is the canonical momentum and $\boldsymbol{\alpha}$ the polarization vector. To result in a non-zero matrix element for the $0 \rightarrow 1$ transition, H_{int} must depend on y since the envelope functions $|0\rangle$ and $|1\rangle$ are represented by functions of y and by plane waves in the other two directions [7]. Choosing the gauge of the vector potential to be $\boldsymbol{A} = (-By, 0, 0)$, we obtain $H_{\text{int}} = (e/m^*)\,\alpha_x(p_x - eBy)$ for the polarization $\boldsymbol{\alpha} = \alpha_x$. Hence, for this polarization we find that

$$\langle 1 | H_{\text{int}} | 0 \rangle_x = \frac{e}{m^*}\,\alpha_x eB \langle 1 | y | 0 \rangle . \tag{1}$$

The transition probability $w = |\langle 1 | H_{\text{int}} | 0 \rangle|^2$ is therefore proportional to the square of the magnetic field for the cyclotron-resonance active polarization $\boldsymbol{\alpha} = \alpha_x$, while it vanishes for the polarization parallel to the magnetic field $\boldsymbol{\alpha} = \alpha_z$. In agreement with our experimental findings, there is no absorption at zero magnetic field in the Voigt geometry. From (1) we find that the absorption for light polarized in the x-direction is proportional to the square of the matrix element for the transverse light polarization M_y, with $M_y = \langle 1 | y | 0 \rangle$. The only parameters determining the absorption for $\boldsymbol{\alpha} = \alpha_x$ with the corresponding matrix element M_x are the effective mass m^* and M_y.

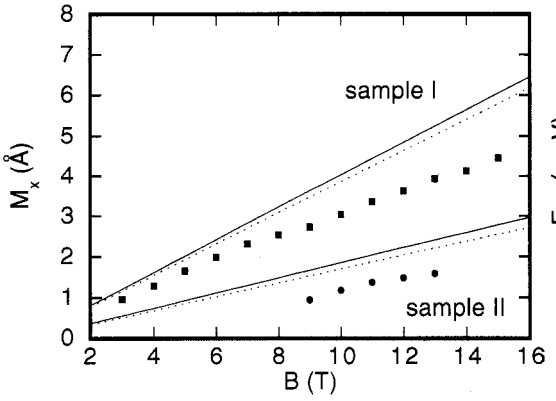

Fig. 2.

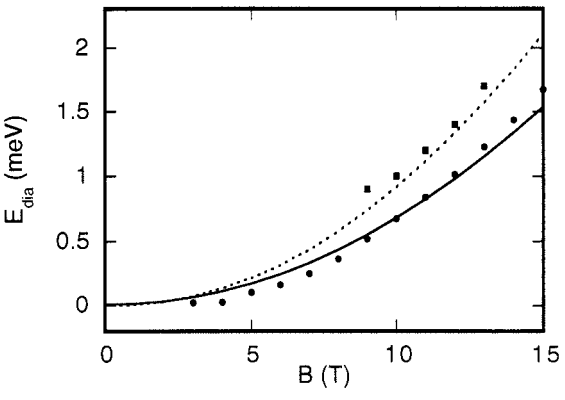

Fig. 3.

Fig. 2. – The matrix element M_x depends to a good approximation linearly on the magnetic field. Since the absolute transmitted signal of sample II is much weaker than for sample I, there are not as many data points. The slope of the data points allows us to deduce the value of M_x while the offset may be caused by the ratio. The calculated $M_x(B)$-dependence describes the data better if the effective optical mass (dotted lines) is used instead of the band edge mass (solid lines). The inset shows schematically the dependence of the spin-split subband energies on the magnetic field and the allowed transitions.

Fig. 3. – Diamagnetic shifts calculated ..... sample I, —— sample II) in an 8-band model and the measured (● sample I, ■ sample II) values agree quite well over the entire field range. Note that the total shift in the transition energy is only approximately 2 meV at $B = 15$ T.

Experimentally, we determine the matrix element M_x from the measured integrated absorption I_A [4] in the Voigt configuration:

$$I_A = \frac{2\pi e^2 N_s n_{Well} \nu}{\varepsilon_0 cn} M_x^2 . \tag{2}$$

Here, ν is the transition frequency, the number of wells is given by n_{Well} and n denotes the refractive index. The other symbols have their usual meaning. In fig. 2, we show the B-dependence of M_x as derived from (2) and see that it does indeed vary linearly with the magnetic field for both samples I and II. This same field dependence has been found before in InAs/AlSb multi-quantum wells as described elsewhere [8]. At all fields the matrix element M_x for the narrower well II is considerably smaller than for well I reflecting a smaller value of M_y.

According to (1) M_y can be found by plotting M_x as a function of B. The values of M_y (a)) given in table II are derived from a fit to the data with the GaAs band edge effective mass

TABLE II.

	Sample I	Sample II
M_y (Å) (calculated)	23.6	17.4
M_y (Å) (tilted angle)	23.5	13.8
a) M_y (Å) (Voigt)	16.9	14.7
b) M_y (Å) (Voigt)	17.7	17.5

$m^* = 0.067 m_0$. Fairly good agreement is reached with measurements under an oblique angle and values calculated self-consistently in the one-band effective-mass approximation. However, the effective mass in eq. (1) is not yet corrected for the conduction band non-parabolicity of GaAs which will be included in an 8-band model.

To this end, we determine the non-parabolic energy dispersion of the AlGaAs/GaAs quantum wells subjected to an in-plane magnetic field from the 8-band Kane-Hamiltonian H_{Kane} as given in [9] using boundary conditions as derived in [10]. In this approach the band-bending is accounted for by first-order perturbation theory. Although the multi-band dispersion is not calculated self-consistently, the eigenenergies and the wave functions at $B = 0$ T are very similar to those obtained in the one-band self-consistent computation. This result can be understood as $E_1 \gg E_F$ for the investigated samples. Solving the Kane-Hamiltonian yields the B- and $k_\parallel$-dependent eigenenergies and an 8-component wave function for each subband. These subbands are spin-split at finite fields as shown schematically in the inset of fig. 2. As the electronic g-factor of GaAs is only small, the energetic difference between the $|\uparrow\rangle$- and $|\downarrow\rangle$-states of the subbands is less than 2.5 meV for both samples even at a magnetic field of $B = 15$ T. In fig. 3, we average the single-particle transition energies over all allowed values of $k_\parallel$ and over both possible spin-conserving transitions and plot it as a function of the magnetic field B. Comparison with the experimentally obtained data shows that the calculated B-dependence of the resonance energy describes the experimental data very well.

In the framework of the same 8-band $k \cdot p$ Hamiltonian we also calculated the matrix elements M_x and M_y using $H_{\text{int}} = eA_0 \sum_i \alpha_i (\partial H_{\text{Kane}})/(\partial P_i)$ [11] with A_0 as the amplitude of the vector potential. For both samples the matrix elements M_y are almost identical to those obtained in the self-consistent calculation and to a good approximation spin-independent. We find again that M_x is proportional to B, whereas the value of M_y varies only little with the magnetic field. However, the slope of $M_x(B)$ in the multi-band calculation is not as steep as in the one-band model. As shown in table II *b*) this more sophisticated calculation yields far better agreement with the experiment as compared to the simple one-band analysis given above. The change in slope can be interpreted as an increase of the electronic mass with energy caused by the conduction band non-parabolicity in GaAs [12]. To test this interpretation we evaluate eq. (1) using an effective mass of $m^* = 0.07 m_0$ for sample I and $m^* = 0.073 m_0$ for sample II and reach the very same slopes as $M_x(B)$ as in the $k \cdot p$ approach. This change in the effective mass m^* is illustrated by plotting $M_x(B)$ with the band edge mass and the mass corrected for non-parabolicity effects, respectively (fig. 2). In this figure only the slopes of the theoretical curves and the data points may be compared as the offset may be caused by base-line problems in the ratioed spectra. We find that the non-parabolicity corrected mass (dashed lines) gives a slope that describes the data points better than the band edge mass (solid lines). The values for m^* can thus be considered to represent an effective optical mass which determines the oscillator strength of the transition. As expected theoretically, this effective optical mass turns out to be lower for the wider well I with the smaller carrier density than for the narrow well II.

Another issue we would like to discuss is the influence of the depolarization effect on our experiments. It is well known that ISR driven by a transverse electric field are subject to a depolarization field [3] resulting in a shift of the transition energy and a narrowing of the linewidth [13]. In our case, however, the resonance positions of the experiments in the Voigt configuration for $B \to 0$ T (fig. 1*b*)) and the measurements under oblique incidence (fig. 1*a*)) give almost the same transition energies. Since the depolarization shift is estimated to be 5 meV for both samples, the resonances of the Voigt geometry experiment must also be affected by the depolarization even at vanishingly small magnetic fields. This can be

understood as in the Voigt configuration the absorbed light is no longer transverse but has a finite component along the growth direction [14]. This electric-field component turns out to be proportional to the magnetic field B [14] giving an absorption proportional to B^2.

We may add that related experiments have been carried out on Si MOS structures [15] in tilted magnetic fields and on InSn MOS structures [16] in the Voigt configuration. In both these cases, however, the magnetic-field dependence of the resonance could not be studied over a wide range, since the subband spacings for both structures are comparable to the cyclotron energy even at moderate fields. Furthermore, the self-consistent triangular potential obscures the B^2-dependence of the oscillator strength.

In summary, we have observed optical transitions between hybrid magneto-electric subbands on AlGaAs/GaAs quantum wells in the Voigt configuration. The in-plane magnetic-field dependence of the oscillator strength allows us to determine the relevant matrix elements and the effective optical mass of the transition with high accuracy. The diamagnetic shift of the subbands as determined from the magnetic-field–dependent transition energy can be quantitatively described in the framework of an 8-band Kane-Hamiltonian.

* * *

We gratefully acknowledge valuable discussions with W. ZAWADZKI. Financial support from the Volkswagen is also gratefully acknowledged.

REFERENCES

[1] ROSENCHER E., VINTER B. and LEVINE B. (Editors), *Intersubband Transitions in Quantum Wells, NATO ASI Series* (Plenum Press, New York, N.Y.) 1992.
[2] CHUI H. G., LORD S. M., MARTINET E., FEIJER M. M. and HARRIS jr. J. S., *Appl. Phys. Lett.*, **63** (1993) 364.
[3] ANDO T., FOWLER A. B. and STERN F., *Rev. Mod. Phys.*, **54** (1982) 481.
[4] WEST L. C. and EGLASH S. J., *Appl. Phys. Lett.*, **46** (1985) 1092.
[5] HEITMANN D. and MACKENS U., *Phys. Rev. B*, **33** (1986) 8269.
[6] LEVINE B. F., MALIK R. J., WALKER J., CHOI K. K., BETHEA C. G., KLEINMAN D. A. and VANDENBERG J. M., *Appl. Phys. Lett.*, **50** (1987) 273.
[7] ZAWADZKI W., *Semicond. Sci. Technol.*, **2** (1987) 550.
[8] GAUER C., WIXFORTH A., KOTTHAUS J. P., KUBISA M., ZAWADZKI W., BRAR B. and KROEMER H., to be published in *Phys. Rev. Lett.*
[9] ZAWADZKI W., KLAHN S. and MERKT U., *Phys. Rev. B*, **33** (1986) 6916.
[10] BURT M. G., *Semicond. Sci. Technol.*, **3** (1988) 739.
[11] SUZUKI K. and HENSEL J. C., *Phys. Rev. B*, **9** (1974) 4184.
[12] WARBURTON R. J., MICHELS J. G., NICHOLAS R. J., HARRIS J. J. and FOXON C. T., *Phys. Rev. B*, **46** (1991) 13394.
[13] ZALUZNY M., *Phys. Rev. B*, **43** (1992) 4511.
[14] ZAWADZKI W., *Adv. Phys.*, **23** (1974) 435.
[15] BEINVOGL W. and KOCH J. F., *Phys. Rev. Lett.*, **40** (1978) 1737.
[16] OELTING S., MERKT U. and KOTTHAUS J. P., *Surf. Sci.*, **170** (1986) 402.